CONF-910418

LA-UR 90-4354

Received by OSTI

JAN 0 8 1991

LA-UR--90-4354

DE91 005901

TITLE: FRACTURE-LINING MINERALS IN THE LOWER TOPOPAH SPRING TUFF AT YUCCA MOUNTAIN

AUTHOR(S): Barbara A. Carlos, David L. Bish, and Steve J. Chipera

SUBMITTED TO: 1991 American Nuclear Society Meeting
April 1991
Las Vegas, NV

Los Alamos
Los Alamos National Laboratory
Los Alamos, New Mexico 87545

FRACTURE-LINING MINERALS IN THE LOWER TOPOPAH SPRING TUFF AT YUCCA MOUNTAIN

Barbara A. Carlos
Geology/Geochemistry Group
EES-1, MS D462
Los Alamos National Laboratory
(505) 667-6879

David L. Bish and Steve J. Chipera
Geology/Geochemistry Group
EES-1, MS D469
Los Alamos National Laboratory
(505) 667-1110

ABSTRACT

Fracture-lining minerals in the lower Topopah Spring Member of the Paintbrush Tuff at Yucca Mountain, Nevada, are being examined to characterize potential flow paths within and away from the candidate repository horizon. Fracture coatings within this interval can be divided into five categories based on rock matrix and type of fracture. Fracture coatings in the densely welded tuff above the basal vitrophyre, near the candidate repository horizon, include (1) those related to lithophysal cavities; (2) mordenite and manganese oxides on nearly planar fractures; (3) later fracture coatings consisting of zeolites, smectite, and calcite. Fracture-coating minerals in the vitrophyre are fine-grained and consist of smectite and a variety of zeolites. The non- to partially-welded vitric and/or zeolitic tuff below the vitrophyre contains fractures mostly lined by cristobalite and clinoptilolite.

INTRODUCTION

Yucca Mountain, in southwest Nevada (Fig. 1), is being studied as a candidate for the nation's first high-level nuclear waste repository. Yucca Mountain is a fault block consisting of more than 1000 m of silicic tuffs and lavas, of which the Paintbrush Tuff is the uppermost unit. The lower portion of the Topopah Spring Member of the Paintbrush Tuff, which is everywhere above the static water level at Yucca Mountain, is the candidate repository horizon. During preliminary geologic studies of Yucca Mountain, several holes were drilled in and around the mountain. Cores from five of these holes have been examined to determine the distribution of fracture-lining minerals as part of characterization of the minerals along potential transport pathways. Minerals lining fractures along these potential pathways are of particular importance as they would likely interact with any fluids passing through the repository host rock. Of particular interest are the minerals in the portion of the Topopah Spring Member nearest the candidate repository horizon. Samples from the partially cored water well J-13, where the Topopah Spring Member is partially below the static water level, were also studied for comparison with core from Yucca Mountain.

METHODS

Cores were examined, and 15-30 representative samples containing fractures were selected from the lower part of the Topopah Spring Member from each of five drill holes: USW G-1, USW G-2, USW GU-3, USW G-4, and UE-25a#1 (Fig.1). Fracture coatings were examined using a binocular microscope, and subsamples were taken for thin-section and

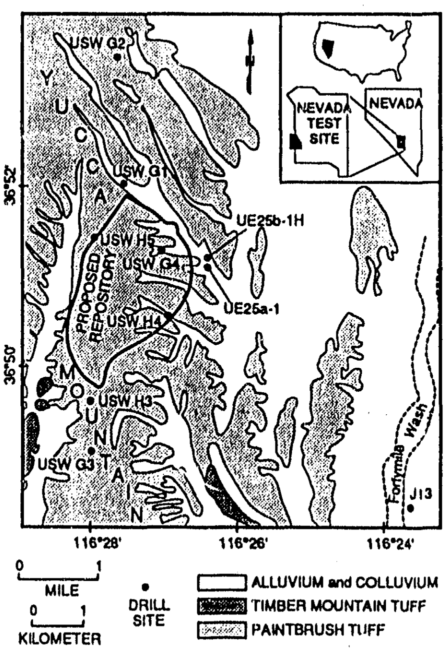

Figure 1. Map showing locations of proposed repository and drill holes.

scanning electron microscope (SEM) studies. Samples for x-ray powder diffraction (XRD) analysis were scraped from the fracture surfaces and were handpicked under the binocular microscope to remove rock matrix contamination. XRD analyses were obtained with an automated Siemens D-500 powder diffractometer using Cu Kα radiation. Mineral analysis was accomplished by comparison with JCPDS and in-house standard patterns. Results of the XRD analyses are given in Table I. All sample numbers in Table 1 represent depth in feet. SEM studies were made using an ISI model DS-130 SEM operated between 15 and 25 KeV. Qualitative energy dispersive (EDS) analyses were obtained with the SEM and Tracor Northern software.

STRATIGRAPHY

The Topopah Spring Member in these drill holes is essentially comprised of an upper quartz latitic cap rock, which may or may not contain a vitrophyre; an upper lithophysal zone with round lithophysal cavities; a middle moderately welded non-lithophysal zone; a lower lithophysal zone with larger flattened lithophysal cavities; a lower densely welded non-lithophysal zone; a lower vitrophyre; and below that, a basal non- to moderately-welded vitric and/or zeolitic tuff. The candidate repository horizon is the densely welded tuff above the lower vitrophyre, possibly including part of the lower lithophysal zone. Core samples were therefore selected from the lower lithophysal zone to the base of the Topopah Spring Member. The stratigraphy of the drill cores has been described by the U. S. Geological Survey,[1,2,3,4,5] and the detailed petrography of the Topopah Spring Member is discussed by Byers and Moore.[6] Static water levels (SWL) are from Fig. 6 in Byers and Moore.[6] Fig. 2 shows the generalized stratigraphy of the Topopah Spring Member in the five drill cores studied, the intervals sampled, and the SWL in each drill hole. USW G-4 was sampled in its entirety because it is closest to the candidate exploratory shaft. The drill holes in Fig. 2 are presented with the southernmost on the left. Drill hole UE-25a#1 is east of Yucca Mountain. Faults between the drill holes are not indicated on Fig. 2, but they affect both the surface elevation and the depths at which stratigraphic units are intersected. The major occurrences of fracture coatings for each drill core are also indicated on Fig. 2. Fracture coatings depicted on Fig. 2 above the sampled intervals were determined by inspection of core photos and brief examination of whole core at the core library. Fracture-lining minerals in the Topopah Spring Member in drill hole USW G-4 and those in water well J-13 were discussed previously in Los Alamos reports.[7,8]

RESULTS

A. Fracture-Lining Minerals Above the Vitrophyre

From the five cored holes on and near Yucca Mountain, a general sequence of mineral deposition in fractures in the devitrified tuff above the vitrophyre can be derived. The first-formed fractures are physically connected to lithophysal cavities and originally contained tridymite, which may or may not now be transformed to cristobalite or quartz. They are designated lithophysal fractures and are identified by bleached (altered) zones extending into the matrix away from the fractures and by the tridymite morphology, which is preserved in pseudomorphs of cristobalite and quartz. These fractures also may contain minor amounts of vapor phase minerals such as hematite. Lithophysal fractures cannot always be distinguished from lithophysal "breaks," which occur when the lithophysal cavity is larger in diameter than the drill core. The lithophysal cavities are more likely to contain later minerals than the near-vertical segments of these fractures.

The second fractures to form were smooth, nearly planar features, which may be cooling fractures. Manganese oxides are often the first coatings on these fractures, occurring as dendrites or small (<1 mm) radiating crystal aggregates. The tabular manganese minerals rancieite [$(Ca,Mn)Mn_4O_9 \cdot 3H_2O$] and lithiophorite [$(Al,Li)MnO_2(OH)_2$] have both been identified in these fractures. The tunnel-structure manganese oxide todorokite [$(Na,Ca,K)_{0.5}Mn_6O_{12} \cdot 4H_2O$] is also present. The XRD patterns of lithiophorite and todorokite are very similar, and we therefore have relied primarily on chemistry and morphology to distinguish between the two. Fibrous manganese oxides have been observed in some SEM images and Ba is present in EDS spectra of manganese oxide crusts, in which no crystal morphology can be distinguished at 3000x magnification, suggesting the presence of todorokite. Fine-grained mordenite forms crusts in these fractures, often over the manganese oxides. The less-common occurrence of manganese oxides over mordenite may be a result of manganese oxides from the other side of the fracture adhering to the mordenite when the fracture was re-opened during coring. Both manganese oxides and mordenite occur as discontinuous patches on the surfaces of the fractures. In some fractures, slickensides are well developed on these coatings. Non-lithophysal quartz occurs on some of these planar fractures, usually parallel to the fracture and with a flattened shape because of constricting fracture walls.

Rougher fractures above the vitrophyre appear to have formed after the two types described above. Coarse-grained zeolites, including stellerite ($CaAl_2Si_7O_{18}•7H_2O$), heulandite/clinoptilolite, and mordenite appear to have formed after and do not occur as high up in the stratigraphic section as the fine-grained mordenite that occurs in the planar fractures. The XRD pattern for stellerite is very similar to that of stilbite [$NaCa_2(Al_5Si_{13}O_{36})•14H_2O$]; however, the presence of stellerite rather than stilbite was determined by the orthorhombic crystal morphology and the absence of Na in the EDS spectra. The XRD pattern for heulandite is the same as that of clinoptilolite because the two minerals are isostructural. The two minerals can be most readily distinguished by heating to 450°C,[9] but heating experiments were not conducted for most of these samples. Results of heating experiments on heulandite/clinoptilolites from USW G-4[7] showed that most samples from above the vitrophyre were intermediate between heulandite and clinoptilolite, falling into type 2 of Boles.[9] Both tabular and prismatic crystals were observed in this interval, and it has not been determined whether all are heulandite or if clinoptilolite is present in some samples. There is great variability in the coarse-grained zeolitic coatings across the mountain, both in the minerals present and in the stratigraphic interval at which they occur. Drill core from USW G-2 contains mordenite, heulandite, and stellerite in the lower lithophysal zone as well as in the lower non-lithophysal zone. It is the only drill core that contains zeolites in lithophysal cavities. In USW G-1 and USW G-4, heulandite and mordenite occur in the lower non-lithophysal zone about 2(m above the vitrophyre. USW G-1 contains stellerite with the heulandite, but stellerite is not as abundant as in USW G-2. Stellerite was not identified in USW G-4. Sampling in UE-25a#1 began only 10 m above the vitrophyre, and heulandite and mordenite are present in the highest sample examined. In USW GU-3, coarse-grained zeolites do not occur in fractures in devitrified tuff above the vitrophyre.

Smectite occurs in all drill cores, but its abundance varies. It usually is a late-formed mineral resembling a dusting of white powder on slickensides, zeolites, or otherwise uncoated fracture surfaces. Smectite is a major fracture coating in USW G-1, where it occurs as rosettes 5-10 µm in diameter or as single "petals" up to 40-µm across, but it is not as abundant in the other drill holes. Even where smectite is a major constituent of the fracture coating, there is not sufficient material nor is the smectite sufficiently rich in K to obtain K/Ar ages.

Calcite commonly appears to be the last mineral deposited wherever it occurs, and its distribution across the mountain is variable. Calcite partially fills lithophysae in USW GU-3, USW G-4, and USW G-2; in the latter hole, it occurs in at least two generations separated by heulandite deposition. Calcite also occurs in lithophysal and other fractures in the lithophysal zones and just above the vitrophyre. The U.S. Geological Survey is currently analyzing stable and radioactive isotopes of the fracture-filling calcites. Coarse-grained coatings of zeolites, smectite, and calcite may also occur in lithophysal or planar (cooling) fractures on top of the original fracture-lining minerals.

Drusy quartz is found only in USW GU-3 at Yucca Mountain, but it is abundant in that drill hole, occurring over tridymite or pseudomorphs after tridymite in lithophysal fractures. Fluorite also occurs in several fractures in USW GU-3 but not in the other holes, and it appears to have been deposited after tridymite and quartz and before calcite.

Samples from water well J-13 were examined for comparison with the Yucca Mountain samples because part of the Topopah Spring Member in J-13 is below the static water level. Lithophysal fractures are the most abundant type above the water table in this hole. Small crusts of fine-grained mordenite also occur. Below the static water level, partially dissolved euhedral drusy quartz is the most abundant fracture coating. No heulandite was identified above the vitrophyre in this hole.

B. Fracture-Lining Minerals in the Vitrophyre

Fractures in the vitrophyre are often nearly vertical, closely spaced, and nearly planar. Most contain a very fine-grained white-to-orange coating that contains heulandite, smectite, and, in some fractures, mordenite. Isolated occurrences of other zeolites were found. Erionite has been identified in a fracture in the vitrophyre in UE-25a#1 and immediately above the vitrophyre in USW GU-3 and USW G-4. The only phillipsite identified to date at Yucca Mountain occurs in UE-25a#1 in a fracture only a meter deeper than the erionite in that core. All other fractures sampled from the vitrophyre in UE-25a#1 contain heulandite and smectite. Chabazite was identified in one sample from the vitrophyre in J-13. Lobate dendrites of manganese oxide minerals occur under the heulandite-smectite coatings in all holes. Rancieite and lithiophorite are the only manganese oxide minerals positively identified to date.

C. Fracture-Lining Minerals Below the Vitrophyre

Heulandite and/or clinoptilolite and opal-CT and/or cristobalite are the predominant fracture-coating minerals below the vitrophyre, whether the matrix is vitric or zeolitic. Fractures are not abundant, and the

Table I. Qualitative Mineralogy as Determined by XRD for USW G-1 Fracture Samples

USW G-1 Sample	Smectite	Heulandite[1]	Stellerite	Quartz	Cristobalite	Opal-CT	Tridymite	Feldspar	Rancieite	Lithiophorite	Other
1104.3/1104.5	Trace	---	---	Major	Minor	---	Minor	Minor	---	---	Hematite[4]
1156.0/1156.4	Major	Trace[2]	---	Major	Minor	---	Minor	Minor	---	---	Hematite[5]
1165.5/1165.8	Major	Trace[2]	---	Major	---	---	Minor	Major	Minor[3]	Major[11]	Hematite[5]
1225.6/1225.9	Major	Trace	Major	Minor	---	---	---	Minor	---	---	
1281.8/1282.0	Trace	Major	???[7]	Trace	Minor	---	---	Trace	---	---	Calcite[6]
1297.0/1297.2	Major	---	---	Minor	---	Major	---	Minor	Trace[3]	---	
1337.0/1337.5	Major	Major	---	Minor	---	Major	---	Minor	Minor[3]	---	
1356.0/1356.3	Trace	Major	---	Minor	---	Major	---	Minor	---	---	

USW G-2 Sample	Smectite	Heulandite[1]	Mordenite	Stellerite	Quartz	Cristobalite	Opal-CT	Tridymite	Feldspar	Lithiophorite	Other
1178.4/1178.7	Trace	---	---	---	Major	---	---	Minor	Trace	---	Hematite[4]
1282.0/1282.1	Trace	---	Trace[2]	---	Major	---	---	Major	Minor	---	Hematite[5]
1447 lithoph	Minor	---	Minor	---	Minor	Major	---	Minor	Major	---	Hematite[5]
1447 breccia	Minor	Minor	Minor	???[7]	Major	Major	---	Trace	Major	---	Hematite[4] Calcite[6]
1449	Minor	Major	Major	Major	Minor	???[8]	---	---	Minor	---	
1456	Trace	Trace	Major	---	Minor	???[9]	---	Trace	Minor	---	
1488.2	Minor	---	Trace	???[7]	Major	---	---	???[8]	Minor	---	Hematite[4]
1505.0/1505.2	Minor	Trace	Major	Major	Major	???[8]	---	???[8]	Trace	---	
1516.7/1517.0	Trace	---	Major	Major	Minor	???[8]	---	---	Minor	---	
1534.4	Trace	Trace	Major	Trace	Minor	Minor	---	---	Minor	---	
1568.8/1569.2a	Trace	Major	Minor	Major	Trace	Minor	---	---	---	---	
1568.8/1569.2b	Trace	Major	Trace	Major	Major	Minor	---	---	---	---	
1581.0/1582.2	Trace	Minor	Major	Major	Minor	???[8]	---	---	Minor	---	
1603.6/1604.0	Minor	Major	Major	???[7]	Minor	???[8]	---	---	Trace	Major	Trace[3]
1629.7/1630.0	Minor	Major	Trace?	???[7]	Minor	Minor	---	---	Minor	---	
1631.2/1631.4	Major	---	Trace	---	Major	Major	---	---	Major	Minor[11]	Trace[3]
1636.7/1636.8	Major	Minor	---	---	Trace	---	---	---	---	---	
1643.8/1644.0	Major	Minor	---	---	---	---	---	---	---	---	
1653.4	Major	Major	---	???[7]	Trace	---	Minor	---	Trace	---	
1669	Major	Major	Trace	---	---	---	Major	---	Trace	---	
1680.7	Minor	Major	---	---	Minor	---	Major[10]	---	---	---	Trace[3]
1687.6	Minor	Major	Trace	---	Minor	---	Major	---	Trace	---	

USW GU-3 Sample	Smectite	Heulandite[1]	Mordenite	Quartz	Cristobalite	Opal-CT	Tridymite	Feldspar	Rancieite	Lithiophorite	Other
799.7/800.0	Minor	---	---	Major	???[9]	---	Minor	Minor	---	---	Hematite[5]
811.0/811.1	Major	---	Trace[2]	Major	Minor	---	Minor	Minor	---	---	Hematite[4]
818.6/819.0	Major	---	---	Major	???[9]	---	Minor	Minor	Trace[3]	Major	Hematite[5]
829.4/829.8a	---	---	---	Trace	---	---	---	Trace	---	---	Calcite[5] Palygorskite[6]
829.4/829.8b	Trace	---	---	Minor	Minor	---	---	Trace	---	---	Calcite[6]
846.0/846.2	---	---	---	Major	---	---	Minor	Trace	---	---	
876.0/876.2	Trace	---	---	Major	---	---	---	Minor	---	---	Hematite[4]
944.5/944.9	---	---	---	Major	---	---	Major	Minor	---	Trace	Hematite[4]
973.0/973.1	---	---	---	Major	---	---	Minor	Trace	---	---	
976.0/976.5	Major	---	---	Minor	Minor	---	Minor	Minor	---	Minor	Hematite[4]
981.0/981.5	Major	---	---	Major	???[9]	---	Major	Minor	Trace[3]	Minor	
987.5/988.0	Minor	---	---	Major	Minor	---	Major	Major	---	Minor	Hematite[5]
1162.7/1163.0	Major	---	Minor	Minor	Trace	---	---	Minor	Trace[3]	---	Hematite[4]
1189.3/1189.6	Minor	Major	---	Major	---	Minor	---	Trace	Trace[3]	---	Erionite[5]
1210.2/1210.6	Major	---	Trace[2]	Minor	Minor	---	---	Minor	Trace[3]	---	Fluorite[6]
1232.0/1232.1	Major	---	---	---	Minor	---	---	Trace	Trace[3]	---	Fluorite[6]

Table I (cont'd.)

USW G-4 Sample	Smectite	Heulandite[1]	Mordenite	Quartz	Cristobalite	Opal-CT	Tridymite	Feldspar	Rancieite	Lithiophorite	Other
349.0.349.3	Minor	---	Major	---	Minor	---	Minor	Major	---	---	Hematite[4]
669.9/670.3	Trace	---	---	Trace	Trace	---	---	Trace	---	---	Calcite[6]
777.8/778.0	Trace	---	---	Major	???[9]	---	Major	Minor	---	---	Hematite[4]
810.7/811.2	Major	---	Major	Minor	---	---	---	Trace	---	---	
887.2/887.4	Minor	---	---	Major	???[9]	---	Minor	Major	---	---	Hematite[4]
984.0/984.4	Trace	---	---	Major	???[9]	---	Minor	Minor	---	---	Hematite[4]
1001.4/1001.8	Minor	---	---	Major	Minor	---	Trace	Major	---	---	Hematite[5]
1008.1/1008.3	Trace	---	Minor[2]	Major	Minor	---	---	Major	---	---	Hematite[5]
1038.0/1038.7	Major	---	Trace	Major	Minor	---	Major	Major	---	---	Hematite[4]
1072A Fract #1	---	---	---	Major	---	---	Minor	Minor	---	---	Hematite[4]
1072B Fract #2	Minor	---	Minor	Major	Minor	---	Minor	Major	---	---	Hematite[4]
1083 Fract#3	Major	---	---	Minor	Major	---	Major	Major	---	---	Hematite[4]
1148.2/1148.4	Major	---	---	Major	Minor	---	---	Major	---	---	
1160.1/1160.2	Trace	---	---	Major	Minor	---	Trace	Major	---	---	
1173.0/1173.2	Trace	---	Major	Minor	Minor	---	---	Major	---	---	
1201.6/1201.8	Trace	---	---	Major	???[9]	---	Minor	Major	---	Minor	Hematite[4]
1244.5/1244.8	Minor	---	---	Major	Minor	---	---	Major	---	---	Hematite[4]
1254 Fract#1	Trace	Major	Minor	Minor	Minor[10]	---	---	Major	---	---	
1254 Fract#3	---	Major	Trace	Minor	Minor[10]	---	---	Major	---	Minor	
1258.0/1258.1	Minor	Major	---	Minor	Minor[10]	---	---	Minor	Trace	Minor	
1309.0/1309.4	---	Major	---	---	---	---	---	---	---	---	
1341 Blue	Minor	Major	Trace	---	---	Minor	---	---	---	---	
1341 Beige	Minor	Major	---	---	---	Minor	---	---	---	---	
1341 Cream	Major	Minor	---	---	---	Minor	---	---	---	---	
1350.1/1350.3	Major	Major	Trace	Trace	---	Trace	---	---	Trace	---	
1362.1/1362.3	Major	Minor	Trace	---	---	Minor	---	Trace	---	---	
1381.2/1381.5	---	Major	Trace	Trace	---	Major	---	---	---	---	

Ue25a#1 Sample	Smectite	Heulandite[1]	Mordenite	Erionite	Phillipsite	Quartz	Opal-CT	Feldspar	Rancieite
1242.7/1243.1	---	Major	Minor	---	---	Minor	Minor	---	---
1252.3	Trace	Minor	Major	---	---	Minor	Minor	Minor	---
1274.5	Major	Major	Trace	---	---	Minor	Minor	Minor	Trace[3]
1276.0/1276.2	Major	Minor	Minor	---	---	Minor	Minor	Minor	Trace[3]
1282.6	Major	Major	Trace	---	---	---	---	---	Trace?[3]
1296.2	Minor	Major	---	Major	---	---	---	---	---
1301.5/1302.0	Minor	Major	---	---	Major	Trace	---	---	Trace[3]
1309.0/1309.2	Minor	Major	---	---	---	---	Minor	Trace	Trace[3]
1318.4/1319.5	Trace	Major	Minor	---	---	Trace	Minor	---	---
1322.9/1323.2	Minor	Major	Minor	---	---	Trace	Minor	Minor	---
1339.5/1339.7	Minor	Major	Major	---	---	Trace	Trace	Trace	---
1361.8/1362.0	Minor	Major	Minor	---	---	Trace	Major	Minor	---

J-13 Sample	Smectite	Heulandite[1]	Mordenite	Quartz	Cristobalite	Opal-CT	Tridymite	Feldspar	Hematite	Other
800	Major	---	---	Minor	???[9]	---	Major	Major	Trace	---
1101	---	---	Trace[2]	Major	---	---	---	Minor	Trace	Lithiophorite[6,3]
1102	---	---	---	Major	---	---	---	Trace	Trace	---
1345	Trace	Major	---	Trace	---	Major	---	Trace	---	Chabazite[6]
1456	Minor	Major	Minor	???	---	Major	---	???	---	---
1519	Trace	Major	Major	Minor	---	Minor	---	Minor	---	---

[1] Clinoptilolite/heulandite group mineral
[2] Zeolite -- unknown whether heulandite/clinoptilolite or mordenite
[3] Rancieite believed to be present based on chemistry and a single XRD reflection
[4] Trace amount [5] Minor amount [6] Major amount
[7] Presence uncertain due to peak overlaps with heulandite and mordenite
[8] Presence uncertain due to peak overlaps with stellerite
[9] Presence uncertain due to peak overlaps with feldspar or tridymite
[10] Either poorly crystallized cristobalite or opal-C
[11] Probably todorokite rather than lithiophorite based on SEM analyses

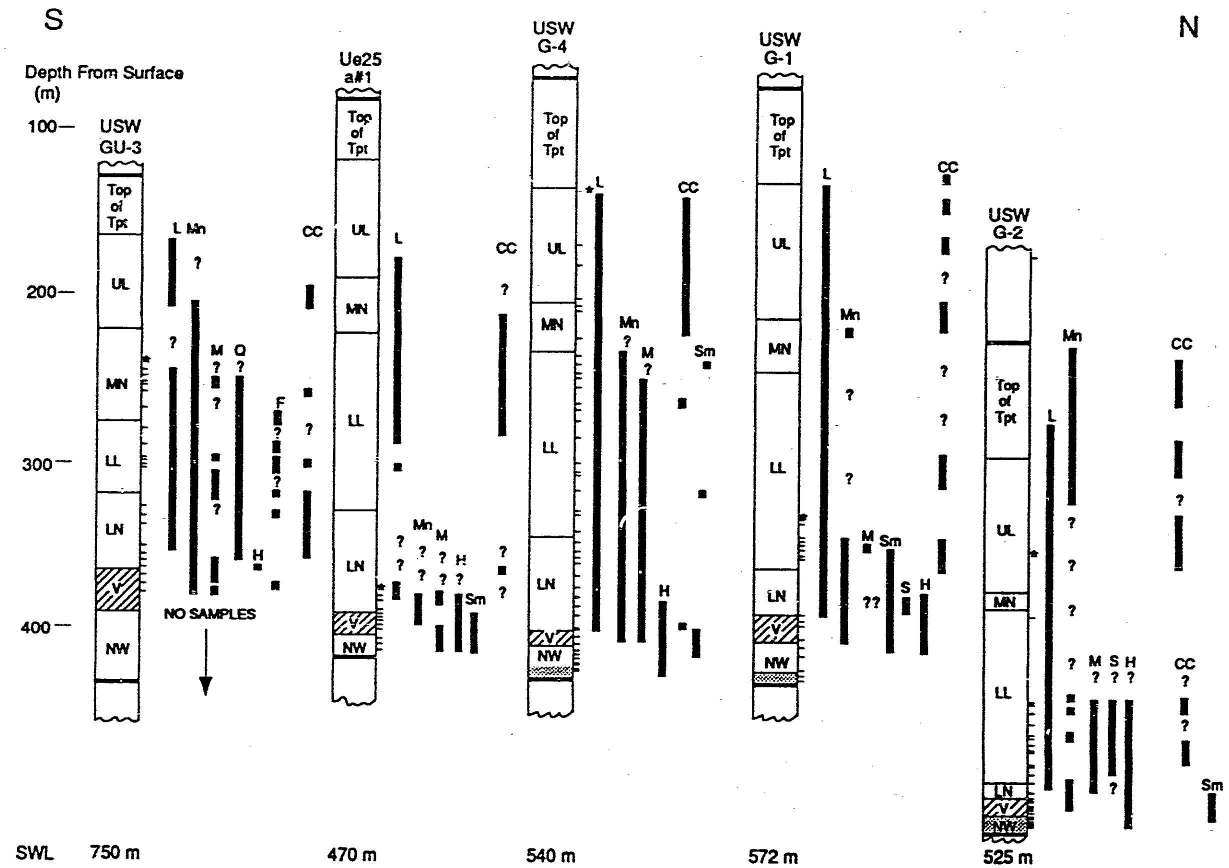

Figure 2. Generalized stratigraphy of four drill holes, arranged roughly from south (left) to north (right) at Yucca Mountain. Depths are from surface, which is a different elevation for each drill hole. UL = upper lithophysal, MN = middle non-lithophysal, LL = lower lithophysal, LN = lower non-lithophysal, V = vitrophyre, NW = non-welded, SWL = static water level (depth in hole). Stipple indicates zeolitic part of non-welded interval. * marks top of sampled interval. Samples are indicated by tick marks. Fracture mineralogy is indicated by bars showing distribution of major abundances of the mineral. *L* = lithophysal, MN = manganese, M = mordenite, Q = quartz, H = heulandite, S = stellerite, SM = smectite, CC = calcite, F = fluorite.

coatings do not appear continuous on open fracture surfaces, perhaps because the core did not always break along pre-existing fractures. Mordenite and manganese oxides were seldom seen in this interval in the cores examined.

PARAGENESIS

Our interpretation of the paragenesis of the fracture coatings is based on the observed fracture-mineral stratigraphy and cross-cutting relationships. The lithophysal coatings in fractures and lithophysal cavities appear to have been deposited during degassing and devitrification of the tuff, since lithophysal cavity mineralogy is primarily deposited from the vapor-phase. The planar fractures in the devitrified tuff and possibly in the vitrophyre are probably related to cooling of the tuff unit. The association of the manganese oxides and fine-grained mordenite with cooling fractures suggests that these minerals were deposited during the period of cooling of the Paintbrush Tuff. These fractures are often slickensided; since it is believed that most of the movement at Yucca Mountain took place prior to 11.5 My ago,[10] these coatings likely were formed prior to this time. It is postulated that the coarse-grained zeolites (heulandite, stellerite, and some mordenite) formed after most of the tectonic movement, as these minerals are not slickensided and the euhedral crystals are generally uncrushed. The greater abundance of these zeolites in the northern portion of Yucca Mountain suggests that they may have formed under the higher temperature gradient that existed there, possibly related to the Timber Mountain Caldera, centered a few kilometers north of Yucca Mountain. The Timber Mountain Caldera is the source of the Rainier Mesa Member of the Timber Mountain Tuff, dated at 11 my. The lack of heulandite above the vitrophyre in the southernmost holes USW GU-3 and J-13 suggests that the distribution of heulandite is not related to the present water table (as was previously suspected for J-13[8]). Drusy quartz is the coarse-grained fracture lining in these two holes, and fluorite is abundant in USW GU-3. The ages of the smectite and calcite in the Topopah Spring Member have not been established.

Fracture coatings in the vitrophyre are extremely variable. Zeolites that have not been identified elsewhere at Yucca Mountain were seen in single occurrences in the vitrophyre. The presence of different minerals only a meter apart argues for localized control of fracture-coating mineralogy. Chipera and Bish[11] concluded, based on calculated activity diagrams,[12] that minor changes in silica activity can potentially give rise to abrupt mineralogic changes similar to those seen in the vitrophyre.

The transition from tridymite to quartz in the lithophysal fractures appears to be through an intermediate phase of cristobalite, sometimes recognizable in SEM images by the whiskery appearance of the tridymite (or tridymite pseudomorphs). Micrometer-sized overgrowths of silica are also common. XRD analyses show that the transition is not simply tridymite-cristobalite-quartz; all tridymite does not disappear prior to the formation of quartz. All three phases are commonly present in the lithophysal zone, showing no regular change in proportion with depth until at some point tridymite disappears and only cristobalite and quartz remain. In drill holes USW G-1, USW GU-3, and USW G-4, the tridymite disappears approximately at the top of the lower non-lithophysal zone, but in USW G-2, it is near the top of the lower lithophysal zone. Sample density in all drill holes is not sufficient to identify the exact interval of tridymite disappearance and the appearance of zeolites, but the two are close if not identical. UE-25a#1 was not sampled high enough to encounter tridymite. Tridymite is present above the water table in J-13 but not below it. As that hole was only intermittently cored, it is not possible to determine the relationship of tridymite to lithophysal or non-lithophysal intervals.

SUMMARY AND CONCLUSIONS

Cores from these drill holes demonstrate that fracture mineralogy often differs significantly from matrix mineralogy,[13] especially in the unsaturated zone. Whereas the matrix mineralogy of the Topopah Spring Member is dominated by quartz, cristobalite, and feldspar, the fractures in the candidate repository horizon and immediately below it contain zeolites, smectites, and manganese oxides that can act as natural sorptive barriers to the migration of radionuclides. There is considerable lateral variation north to south along Yucca Mountain in the mineralogy and distribution of these sorptive fracture coatings. Zeolites, especially heulandite/clinoptilolite and stellerite, are more abundant and extend over a larger stratigraphic interval in the north than in the southernmost hole, USW GU-3. Smectite, though present in all cores, is much more abundant in USW G-1 than in the other cores. The manganese oxide minerals rancieite, lithiophorite, and/or todorokite have been identified in all cores. They appear to be more abundant in USW GU-3, but whether there is a general increase in amount to the south or whether this increased abundance is specific to USW GU-3 cannot be determined from the present samples. More holes within the block will be necessary to determine the distribution and abundance of all the potentially sorptive minerals within and adjacent to the candidate repository.

These significant differences between matrix and fracture mineralogy in the candidate repository horizon at Yucca Mountain and the lateral variations in fracture mineralogy emphasize the necessity to characterize the fractures thoroughly. The minerals observed in fractures are generally more sorptive for radionuclides than the matrix mineralogy and may constitute an important natural barrier to the migration of radionuclides as they occur along potential flow paths away from the candidate repository. Complete assessment of the importance of fracture minerals at Yucca Mountain will require a better understanding of the vadose-zone hydrology and the sorptive properties of the individual fracture-lining minerals.

ACKNOWLEDGMENTS

This work was supported by the Yucca Mountain Site Characterization Project Office as part of the Civilian Radioactive Waste Management Program. This Project is managed by the U.S. Department of Energy, Yucca Mountain Project.

REFERENCES

1. F. MALDONADO and S. L. KOETHER, "Stratigraphy, Structure, and Some Petrographic Features of Tertiary Volcanic Rocks at the USW G-2 Drill Hole, Yucca Mountain, Nye County, Nevada," Open-File Report 83-732, U. S. Geological Survey (1983).

2. R. B. SCOTT and M. CASTELLANOS, "Stratigraphic and Structural Relations of Volcanic Rocks in Drill Holes USW GU-3 and USW G-3, Yucca Mountain, Nye County, Nevada," Open-File Report 84-491, U. S. Geological Survey (1984).

3. R. W. SPENGLER, D. C. MULLER, and R. B. LIVERMORE, "Preliminary Report on the Geology and Geophysics of Drill Hole UE25a-1, Yucca Mountain, Nevada Test Site," Open-File Report 79-1244, U.S. Geological Survey (1979).

4. R. W. SPENGLER, F. M. BYERS, JR., and J. B. WARNER, "Stratigraphy and Structure of Volcanic Rocks in Drill Hole USW-G1, Yucca Mountain, Nye County, Nevada," Open-File Report 81-1349, U.S. Geological Survey (1981).

5. R. W. SPENGLER, M. P. CHORNACK, D. C. MULLER, and J. E. KIBLER, "Stratigraphic and Structural Characteristics of Volcanic Rocks in Core Hole USW G-4, Yucca Mountain, Nye County, Nevada," Open-File Report 84-789, U. S. Geological Survey (1984).

6. F. M. BYERS, JR., and L. M. MOORE, "Petrographic Variation of the Topopah Spring Tuff Matrix Within and Between Cored Drill Holes, Yucca Mountain, Nevada," LA-10901-MS, Los Alamos National Laboratory Report (1987).

7. B. A. CARLOS, "Minerals in Fractures of the Unsaturated Zone from Drill Core USW G-4, Yucca Mountain, Nye County, Nevada," LA-10415-MS, Los Alamos National Laboratory Report (1985).

8. B. A. CARLOS, "Fracture-Coating Minerals in the Topopah Spring Member and Upper Tuff of Calico Hills from Drill Hole J-13," LA-11504-MS, Los Alamos National Laboratory Report (1989).

9. J. R. BOLES, "Composition, Optical Properties, Cell Dimensions, and Thermal Stability of Some Heulandite Group Zeolites," American Mineralogist, 57, 1463-1493 (1972).

10. R. B. SCOTT, R. W. SPENGLER, S. DIEHL, A. R. LAPPIN, and M. P. CHORNACK, "Geologic Character of Tuffs in the Unsaturated Zone at Yucca Mountain, Southern Nevada," in Role of the Unsaturated Zone in Radioactive and Hazardous Waste Disposal, J. W. Mercer, P. S. L. Rao, and I. W. Irvine, Eds., Ann Arbor Science, Ann Arbor, Michigan, 289-335 (1983).

11. S. J. CHIPERA and D. L. BISH, "The Occurrence and Distribution of Erionite at Yucca Mountain, Nevada," LA-11497-MS, Los Alamos National Laboratory Report (1989).

12. J. A. CHERMAK and J. D. RIMSTIDT, "Estimating the Thermodynamic Properties (ΔG_f^o and ΔH_f^o) of Silicate Minerals at 298 K from the Sum of Polyhedral Contributions," American Mineralogist, 74, 1023-1031 (1989).

13. D. L. BISH and S. J. CHIPERA, "Revised Mineralogic Summary of Yucca Mountain, Nevada," LA-11497-MS, Los Alamos National Laboratory Report (1989).

END

DATE FILMED

03 / 07 / 91